INSTITUTE FOR SPACE STUDIES

PULSATIONAL INSTABILITIES IN HYDROGEN-POOR

MASSIVE BLUE STARS.   I.

Norman R. Simon

and

Richard Stothers

Institute for Space Studies
Goddard Space Flight Center, NASA
New York
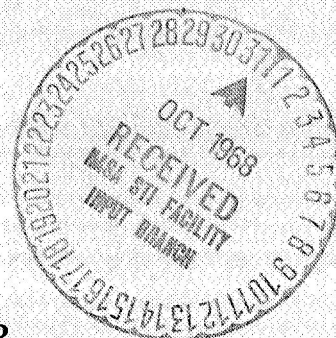
GODDARD SPACE FLIGHT CENTER

NATIONAL AERONAUTICS AND SPACE ADMINISTRATION

PULSATIONAL INSTABILITIES IN HYDROGEN-POOR

MASSIVE BLUE STARS.   I.

Norman R. Simon

and

Richard Stothers

Institute for Space Studies
Goddard Space Flight Center, NASA
New York

ABSTRACT

The structure and pulsational properties of massive stars
with helium cores and thin, hydrogen-poor envelopes have been
investigated. The core structures are very insensitive to
modifications of the hydrogen envelope. However, it is found
that the total stellar radius and luminosity are modified by
the integrated hydrogen content and by the hydrogen gradient,
respectively. The models are pulsationally stable under modest
conditions of central condensation (hydrogen-burning shell and/or
high hydrogen content). The unstable models are energized almost
entirely by the helium reactions in the core, while most of the
damping occurs in the thin, non-burning hydrogen envelope. For
each mass, the period ($\sim$ hour) is remarkably insensitive to the
envelope modifications. The critical models dividing stable
from unstable models are determined by (1) a pulsational eigen-
frequency $\omega^2 \sim 3$ and (2) the value of the hydrogen gradient.
Our critical models explain some of the observed features of
the classical Wolf-Rayet stars of high luminosity but seem to be
too blue with respect to Rublev's sequence of stars on the H-R
diagram.

I. INTRODUCTION

Massive stars on the main sequence become unstable against nuclear-energized pulsations above a certain critical mass (Ledoux 1941; Schwarzschild and Härm 1959). However, evolution off the main sequence quickly stabilizes stars up to the greatest masses (Schwarzschild and Härm 1959). Even when the energy source shifts to a shell outside the contracted helium core, blue stars persist in exhibiting high pulsational stability (Ledoux 1941; Cox 1955; Stothers and Simon 1968). The relevant physical arguments have been amply reviewed in the foregoing references.

All calculations of models so far have been based on the assumption that the stars evolve at constant mass and with developing chemical inhomogeneity. When either or both of these assumptions are relaxed, pulsational instability becomes a greater possibility. As a trivial formal example, consider the evolution of a completely mixed star during hydrogen burning. As hydrogen is depleted throughout the star, the critical mass for instability decreases as the inverse square of the mean molecular weight (Schwarzschild and Härm 1959):

$$M_{crit}/M_\odot = 21\mu^{-2}.$$

A combination of somewhat more complex factors may result in more physically realistic examples. It is therefore of interest

to ask what observational evidence exists for stars of high mass and blue color (because of the necessarily small central condensation) showing a significant degree of instability. The classical Wolf-Rayet stars are certainly prime candidates. However, their evolutionary stage is still a mystery and has been the subject of much discussion. Various proposals have been guided by observational indications placing the stars in different positions with respect to the main sequence, as well as by the relatively low observed masses in binary systems, by some very high luminosities, and by the apparent chemical peculiarities of the stars.

Among the more noteworthy proposals are the following. Pre-main sequence: gravitationally contracting stars (Sahade 1960; Underhill 1966). Main sequence: stars at the end of hydrogen burning (Westerlund 1961, 1964); stars having completely mixed at the end of hydrogen burning and now undergoing substantial mass loss (Westerlund and Smith 1964); pulsationally unstable stars in secondary contraction at the end of hydrogen burning, in analogy with the β Cephei stars (Stothers 1965). Post-main sequence: stars evolved beyond hydrogen burning with substantial loss of mass (Limber 1964; Rublev 1965; Tanaka 1966; Paczynski 1967); stars having completely mixed before, during , or after helium burning (cf. Burbidge, Burbidge, Fowler, and Hoyle 1957);

and stars in the helium-burning stage (Salpeter 1953; Crawford 1953; Divine 1965). Clearly, virtually every possible evolutionary stage has been suggested!

In the present paper, we propose to study the structure and pulsational properties of post-main-sequence stars with massive helium cores and thin, hydrogen-poor envelopes. Pulsational instability (energized by nuclear reactions) may account for the observed variations in many Wolf-Rayet stars. The very high luminosities of some of the stars are assumed in the present work to be the consequence of high mass. Nevertheless, the original masses must have been still greater in order for the stars to have attained the assumed configurations.

II. ASSUMPTIONS

The stellar models under consideration contain three zones:
(1) a radiative outer zone with a smooth gradient of hydrogen
and helium extending from the surface down to a thin shell
(where hydrogen may or may not be burning); (2) a radiative
intermediate zone, devoid of hydrogen, below the shell; and
(3) a convective core where helium burning occurs.

The hydrogen abundance in the radiative outer zone is
assumed to be a linear function of mass fraction

$$X = a_0 + a_1 q \tag{1}$$

where a_0 and a_1 are determined by fixing the hydrogen content
X_R at the surface (q = 1) and requiring X_s = 0.03 at the shell
(q_s). The shell is approximated by a discontinuous jump in
hydrogen and helium as well as in luminosity. For simplicity,
we shall consider only the initial model of helium burning in
the core, so that the helium abundance below the shell may be
represented by Y = 1 - Z, where Z is the metals abundance.
Deinzer and Salpeter (1964) and Boury and Ledoux (1965) have
shown in the case of stars composed of pure helium that little
change in the structure and pulsational properties takes place
as helium is depleted in the core. On this basis we assume that
our results would not be altered much by the choice of a more

evolved core. The metals abundance is taken to be Z = 0.03 throughout our models.

The assumptions adopted here are similar to the ones adopted by Stothers (1966a) and by Stothers and Simon (1968), except that the present models lack a zone of zero-age chemical composition capping the zone of changing composition. The opacity is assumed to be due solely to electron scattering:

$$\varkappa = 0.19 \ (1 + X) \tag{2}$$

The nuclear-energy release is provided by the CNO-cycle in the shell and by the triple-alpha reaction in the core. The rate of the former is given by

$$\varepsilon_H = \varepsilon_H^0 \ X \ X_{CNO} \ \rho \ T^{\nu_H} \tag{3}$$

with

$$X_{CNO} = Z/2, \quad \nu_H = 14, \quad \log \varepsilon_H^0 = -99.0,$$

while the rate of the latter is given by

$$\varepsilon_{He} = \varepsilon_{He}^0 \ Y^3 \rho^2 \ T^{\nu_{He}} \ . \tag{4}$$

The quantities ε_{He}^0 and ν_{He} are allowed to vary from model to model since they are strongly dependent on temperature (Reeves 1965).

III. STABLE MODELS

The masses selected for calculation are 15, 60 and 100 $M_\odot$. The other free parameters which have to be specified are X_R and q_s. The method of calculation has been described in Stothers (1966$\underline{a}$). Results for each mass using a variety of envelope parameters are given in Table 1.

For a given mass, it is found that the luminosity remains approximately constant while the spatial distribution of matter in the star (indicated by the stellar radius or by the radial extension of the shell) varies with the positioning of the shell in mass fraction q_s and with the surface abundance of hydrogen X_R. For increasingly homogeneous models ($q_s \rightarrow 1$), both the total luminosity and the fraction of luminosity contributed by hydrogen burning decrease. Furthermore, the radius fraction of the shell increases with q_s and the total radius decreases. Similar results were found by Cox and Salpeter (1961) for models of stars with much lower masses.

It is useful to differentiate two ways of formally altering the hydrogen content in the envelope: (1) addition of hydrogen, holding the shell mass fraction fixed and (2) reduction of the shell mass fraction, holding the surface hydrogen abundance fixed. In both cases, the integrated hydrogen content $\int X \, dq$

is increased and so is the stellar _radius_. However, the _hydrogen gradient_ dX/dq is steepened in case (1) and reduced in case (2); the stellar _luminosity_ (as well as the hydrogen-burning fraction of the luminosity) decreases and increases, respectively.

For models with a fixed core mass, alterations of the envelope composition have virtually no effect on the structure of the core. Thus, the core is effectively "decoupled" from the envelope and behaves like an isolated star (cf. Hayashi, Hoshi, and Sugimoto 1962).

A comparison of the various masses having the same envelope parameters (X_R, q_s) shows that the fraction of luminosity contributed by hydrogen burning is smaller at the higher masses. Depending on the selected envelope parameters (particularly q_s) this fraction varies from less than 1 percent to nearly 40 percent in our models. However, for any constant set of envelope parameters, the basic stellar quantities show the same trends with mass as do normal main-sequence stars.

On account of the small amount of mass contained in the hydrogen envelopes, our models lie considerably to the left of the core hydrogen-burning main sequence (Stothers 1966b), although, of course, not as far left as the analogous main

sequence for pure helium stars (Deinzer and Salpeter 1964).

Increasing the mass of the hydrogen envelopes still further

can result in location of the models in the blue-supergiant

or even the red-supergiant region (Stothers and Chin 1968;

Stothers and Simon 1968).

IV. PULSATING MODELS

The radial pulsation characteristics of our models were calculated in the usual linear, quasi-adiabatic approximation (Schwarzschild and Härm 1959; Boury and Ledoux 1965; Stothers and Simon 1968). The relative pulsation amplitudes are all continuous through the star, except for the luminosity perturbation which has a discontinuity at the hydrogen shell. The average rate at which energy is being fed into, or removed from, the pulsations over a period is given by

$$L_P = L_{PN} - L_{PH} - L_{PS} \tag{5}$$

where L_{PN} is the rate of gain from nuclear sources, L_{PH} is the rate of flux damping, and L_{PS} is the rate of damping by acoustical waves running off the surface. A positive sign for L_P indicates an unstable configuration. The energizing term L_{PN} contains a contribution both from shell hydrogen burning L_{PN}^s and core helium burning L_{PN}^c, while the main damping term L_{PH} is the sum of the heat loss rate in the envelope L_{PH}^e and in the convective core L_{PH}^c. To avoid the difficulty involved in calculating luminosity amplitudes in a convective region (cf. Boury, Gabriel, and Ledoux 1964), we have estimated them following Schwarzschild and Härm (1959) by means of an average involving quantities computed at

the center and outer boundary of the core only. Such an approximation is sufficient for our purpose because the contribution from these terms is small, never exceeding 30 per cent of the contribution from the surface waves.

The calculated pulsational rates are listed in Table 2 along with the square of the dimensionless frequency

$$\omega^2 = \left(\frac{2\pi}{\text{Period}} \right)^2 \frac{R^3}{GM} \; ; \tag{6}$$

the pulsational $\underline{e}$ - folding time $1/K$, where K is the stability coefficient $(L_p / 2E_p)$ and E_p is the mechanical energy of the pulsations; and the relative pulsation amplitudes at the surface, shell, and center. The quantities with asterisks have been computed without the contribution from surface waves. Otherwise, the notation is the same as in previous papers (Schwarzschild and Härm 1959; Stothers and Simon 1968).

The general conclusions that can be drawn regarding the pulsational eigenfrequencies are already known. For example, ω^2 increases with greater central condensation (as measured by $\rho_c/\bar{\rho}$) and decreases with greater relative radiation pressure (as measured by $1 - \beta_c$). For reference, we note (1) a greater central condensation with increasing radius and (2) a greater relative radiation pressure with increasing luminosity and hence with increasing mass.

The critical value of ω^2 dividing the stable and unstable models
is approximately the same for all masses ($\omega^2 \sim 3$). The reason
is that the critical central condensation increases along with
relative radiation pressure at higher masses (see below and
Appendix). This result for the critical values of ω^2 seems to
be valid not only for our hybrid models but also for pure helium
stars (Boury and Ledoux 1965) and for Population I hydrogen
main-sequence stars (Schwarzschild and Härm 1959).

The pulsation periods of those four models lying in the
vicinity of the critical model for each mass are remarkably
similar. This result is surprising in view of the fact that the
integrated hydrogen abundance and the hydrogen gradient (with
respect to mass fraction) vary by factors up to 6 and 8, respect-
ively. The increase of ω^2 with radius is apparently such that
the period is held nearly constant (eq. [6]).

In all the models, most of the damping comes from heat
leakage in the envelope. The core contributes less than 5 per
cent of the interior damping and the surface waves contribute
less than 20 per cent of the total damping (interior plus surface).
Energizing of the pulsations comes almost entirely from the
helium reactions in the core. The hydrogen shell contributes
less than 10 per cent of the energy for pulsations in all the

unstable models. This is in general due to the fact that L_H/L is small in the unstable models, although the smallness of L_H/L is not a sufficient condition for instability. When the shell is vigorously burning and/or hydrogen is added to the envelope, the envelope is in an expanded state. Such an expansion drives up the central condensation because the central density is fixed at a nearly constant value by the helium-burning reactions. Consequently, the pulsation amplitudes drop off more rapidly inside the surface (see Appendix) and therefore are smaller near the center where most of the destabilization takes place. Hence, a high central condensation tends to induce stability. The critical value of $\rho_c/\bar{\rho}$ dividing the stable and unstable models for each mass is given in Table 3. The corresponding value of $\delta r/r$ at the center is about 40 per cent of the surface amplitude in all cases.

In Table 3 we have also listed the critical value of q_s for each selected mass and surface abundance of hydrogen. An asterisk again indicates that surface waves have been neglected. In general, the deeper the mass fraction of the shell, the less surface abundance of hydrogen is required to induce stability. The key factor determining the critical model for a given mass seems to be the hydrogen gradient rather than the total amount of hydrogen. This is so since the hydrogen gradient determines the degree of central condensation. On account of the smaller

radiation pressure at lower mass, the low-mass models become

unstable under more restrictive conditions on the hydrogen

gradient. In the limit of vanishing hydrogen content (pure

helium stars) the critical mass is 7 to 8 $M_{\odot}$ (Boury and

Ledoux 1965).

V. COMPARISON WITH OBSERVATIONS

The location of Wolf-Rayet stars on the H-R diagram is very uncertain and there is much confusion and argument concerning where they lie with respect to the main sequence. This is true as regards both luminosity and effective temperature. In addition, the masses of these stars are not well known. There are, however, some generally agreed upon properties of Wolf-Rayet stars which are of interest here, although they will be discussed in more detail in a subsequent paper.

First of all, the classical Wolf-Rayet stars are rare objects and must be young because of their close association with O and B stars. Second, these objects seem to be superluminous (as compared with main-sequence stars) for any reasonable masses that are assigned them. Third, many of the stars are surrounded by expanding shells and often by dense, spherically symmetric nebulae. Fourth, their emission lines are frequently observed to vary irregularly on a time scale of hours. Fifth, their electron temperatures are very high and their effective temperatures may also be very hot (possibly hotter than main-sequence stars). Sixth, the atmospheres of these stars seem to be rich in helium and, in the case of the WN sequence, possibly rich in nitrogen as well (as if the surface material had at one time been processed through the CN-cycle).

It has often been suggested in the literature that Wolf-Rayet stars may arise as a result of mass loss. Rublev (1965) states: "It cannot be excluded that WR stars are some sort of remnants of initially very massive stars that have shed a considerable portion of their matter (including all of the hydrogen-rich envelope) and have uncovered layers which during the earlier stages of evolution corresponded to the periphery of the convective core."

The foregoing evidence allows us to make the tentative suggestion that some Wolf-Rayet stars may be massive objects in the core helium-burning stage of evolution and, further, that the structure of these stars could be approximated by our hydrogen-poor, helium-burning models.

Let us examine this suggestion. Figure 1 shows a plot of the H-R diagram of our model stars (open circles), including pulsationally unstable models (crossed open circles). The filled circles represent Wolf-Rayet stars as located by Rublev (1965). The pure helium sequence (Deinzer and Salpeter 1964) and the normal main sequence (Stothers 1966b) along with approximate mass locations are drawn in for reference, at left and right respectively.

It is immediately clear that all Wolf-Rayet stars on the diagram are superluminous, the least luminous star corresponding to a main-sequence mass of about 60 $M_\odot$. This suggests that the Wolf-Rayet stars are not hydrogen-burning, but represent rather a post-main-sequence phase of evolution. If such an evolutionary stage is indeed reached via mass loss on the upper main sequence, then the expanding shells and nebulae which surround Wolf-Rayet stars may be attributed to the ejected matter.

As previously noted, Wolf-Rayet masses are extremely uncertain. Underhill (1966) estimates the average mass in binary systems as lying between 4 and 8 $M_\odot$, while, if one takes Rublev's stars to be burning core helium, his highest mass appears to be $\sim$ 90 $M_\odot$.

Let us turn now to the question of Wolf-Rayet stability. As can be seen in Figure 1, a narrow band of instability exists for our hydrogen-poor models, running close to the pure helium sequence and turning off slightly at high masses. Since Rublev's estimates of effective temperature are higher than most quoted in the literature, it seems unlikely (though still possible) that the Wolf-Rayet locus can be moved any farther to the left. In that case helium core-energized pulsations cannot be the cause of observed variability, since the cooler of our models prove to be quite stable.

It is clear that any mechanism which will account for the present observed properties of luminous Wolf-Rayet stars should also fit in with the previous evolutionary history of mass loss. In a forthcoming paper, we shall propose just such a unified mechanism.

APPENDIX

It is required to show that the gradient of the radius amplitude at the surface is steeper for a higher central condensation. The relevant linearized equations for adiabatic pulsations are

$$x \frac{d}{dx}\left(\frac{\delta r}{r}\right) = -\frac{\delta \rho}{\rho} - 3\frac{\delta r}{r}$$

$$x \frac{d}{dx}\left(\frac{\delta P}{P}\right) = V\frac{\delta P}{P} + V\left(4 + \omega^2 \frac{x^3}{q}\right)\frac{\delta r}{r}$$

$$\frac{\delta P}{P} = \Gamma \frac{\delta \rho}{\rho}, \text{ with } \Gamma = \beta + \frac{2}{3}\frac{(4 - 3\beta)^2}{\beta + 8(1 - \beta)} \quad .$$

At the surface, $x = 1$, $q = 1$, and $V = -d\ln P/d\ln r = \infty$. Therefore, we need the regularity condition

$$\left(\frac{\delta P}{P}\right)_R = -(4 + \omega^2)\left(\frac{\delta r}{r}\right)_R \quad .$$

The gradient at the surface is clearly

$$\frac{d}{dx}\left(\frac{\delta r}{r}\right) = \frac{\omega^2 - (3\Gamma_R - 4)}{\Gamma_R}$$

setting $(\delta r/r)_R = 1$.

We now make use of the well-known variational result (Ledoux and Walraven 1958)

$$\omega^2 \leq (3\bar{\Gamma} - 4) J$$

where the ratio

$$J = \int_0^1 \frac{q}{x} \, dq \bigg/ \int_0^1 x^2 \, dq$$

is a measure of the central condensation, like $\rho_c / \bar{\rho}$. Clearly, ω^2 increases with increasing central condensation and with decreasing relative radiation pressure. As an approximation, we set $\bar{\Gamma} = \Gamma_R$ and use the equality sign in the variational expression for ω^2. Then

$$\frac{d}{dx} \left(\frac{\delta r}{r} \right) = \frac{3\Gamma_R - 4}{\Gamma_R} \left(J - 1 \right).$$

At the stellar surface Γ_R is determined from

$$\beta_R = 1 - (\varkappa_R L / 4\pi cGM).$$

For a given mass and chemical composition, the surface value of β and thus of Γ depends only on the luminosity. But the luminosity is not very sensitive to chemical composition changes

in the envelope. Hence, for a given mass,

$$\frac{d}{dx}\left(\frac{\delta r}{r}\right) \sim J - 1 ,$$

indicating the more rapid drop-off of pulsation amplitudes
(all of which depend on $\delta r/r$) with higher central condensation.

REFERENCES

Boury, A., Gabriel, M., and Ledoux, P. 1964, Ann. d'ap., 27, 92.

Boury, A., and Ledoux, P. 1965, Ann. d'ap., 28, 353.

Burbidge, E. M., Burbidge, G. R., Fowler, W. A., and Hoyle, F. 1957, Rev. Mod. Phys., 29, 547.

Cox, J. P. 1955, Ap. J., 122, 286.

Cox, J. P., and Salpeter, E. E. 1961, Ap. J., 133, 764.

Crawford, J. A. 1953, Pub. A. S. P., 65, 210.

Deinzer, W., and Salpeter, E. E. 1964, Ap. J., 140, 499.

Divine, N. 1965, Ap. J., 142, 824.

Hayashi, C., Hoshi, R., and Sugimoto, D. 1962, Prog. Theoret. Phys. Suppl. (Kyoto), No. 22.

Ledoux, P. 1941, Ap. J., 94, 537.

Ledoux, P., and Walraven, Th. 1958, Hdb. d. Phys., ed. S. Flügge (Berlin: Springer-Verlag), 51, 353.

Limber, D. N. 1964, Ap. J., 139, 1251.

Paczynski, B. 1967, Acta Astr., 17, 355.

Reeves, H. 1965, Stellar Structure, ed. L. H. Aller and D. B. McLaughlin (Chicago: University of Chicago Press), p. 113.

Rublev, S. V. 1965, Astr. Zh., 42, 347.

Sahade, J. 1962, Symposium on Stellar Evolution (La Plata, Argentina: National University of La Plata), p. 185.

Salpeter, E. E. 1953, Ann. Rev. Nuc. Sci., 2, 41.

Schwarzschild, M., and Härm, R. 1959, Ap. J., 129, 637.

Stothers, R. 1965, Ap. J., 141, 671.

_____. 1966$\underline{a}$, ibid., $\underline{143}$, 91.

_____. 1966$\underline{b}$, ibid., $\underline{144}$, 959.

Stothers, R., and Chin, C.-w. 1968, Ap. J., $\underline{152}$, in press.

Stothers, R., and Simon, N. R. 1968, Ap. J., $\underline{152}$, in press.

Tanaka, Y. 1966, Pub. A. S. Japan, $\underline{18}$, 47.

Underhill, A. B. 1966, The Early Type Stars (Dordrecht, Holland:
    D. Reidel Publ.).

Westerlund, B. 1961, Uppsala Ann., $\underline{5}$, No. 1.

Westerlund, B. E. 1964, The Galaxy and the Magellanic Clouds
    (IAU/URSI Symp. No. 20), ed. F. J Kerr and A. W. Rodgers
    (Canberra: Australian Academy of Science), p. 316.

Westerlund, B. E., and Smith, L. F. 1964, M. N. R. A. S., $\underline{128}$,
    311.

TABLE 1

Model Characteristics for Helium-Burning Stars with Hydrogen-Poor Envelopes.

	M = 15 $M_\odot$			
X_R	0.10	0.10	0.05	0.05
q_s	0.95	0.98	0.95	0.97
β_s	0.681	0.708	0.680	0.712
log T_s	7.651	7.518	7.654	7.577
log ρ_s	0.876	0.532	0.882	0.715
r_s/R	0.563	0.661	0.590	0.655
q_4	0.763	0.786	0.763	0.785
β_c	0.592	0.591	0.592	0.591
log T_c	8.287	8.287	8.287	8.287
log ρ_c	2.637	2.636	2.637	2.636
$\rho_c/\bar{\rho}$	34.4	27.7	29.8	25.0
L_H/L	0.089	0.000	0.110	0.004
log $(L/L_\odot)$	5.471	5.440	5.481	5.441
log $(R/R_\odot)$	0.075	0.044	0.054	0.029
log T_e	5.093	5.101	5.106	5.109
ν_{He}	20.0	20.0	20.0	20.0
log ϵ_{He}^0	-164.82	-164.82	-164.82	-164.82

TABLE 1 (continued)

M = 60 $M_\odot$					
0.15	0.15	0.15	0.10	0.05	0.05
0.80	0.95	0.98	0.95	0.90	0.95
0.200	0.372	0.388	0.368	0.247	0.374
7.751	7.685	7.557	7.689	7.743	7.695
0.245	0.421	0.067	0.426	0.338	0.453
0.125	0.487	0.589	0.524	0.332	0.570
0.664	0.879	0.922	0.876	0.770	0.879
0.372	0.347	0.347	0.347	0.354	0.346
8.327	8.333	8.334	8.333	8.331	8.333
2.368	2.339	2.340	2.339	2.346	2.338
3560.	66.8	50.8	53.6	201.	40.6
0.377	0.045	0.000	0.069	0.299	0.075
6.411	6.359	6.355	6.370	6.438	6.374
1.037	0.471	0.431	0.439	0.628	0.399
4.847	5.118	5.136	5.136	5.059	5.157
18.0	17.0	17.0	17.0	18.0	17.0
-148.23	-139.90	-139.90	-139.90	-148.23	-139.90

TABLE 1 (continued)

M = 100 M$_\odot$					
0.15	0.15	0.10	0.10	0.05	0.05
0.95	0.97	0.90	0.95	0.90	0.93
0.289	0.298	0.197	0.291	0.189	0.237
7.691	7.620	7.742	7.698	7.748	7.732
0.274	0.080	0.209	0.300	0.206	0.283
0.463	0.523	0.287	0.517	0.340	0.454
0.894	0.924	0.796	0.895	0.792	0.842
0.279	0.278	0.284	0.278	0.284	0.280
8.348	8.349	8.346	8.348	8.346	8.347
2.245	2.246	2.251	2.245	2.249	2.246
83.7	69.2	329.	58.9	196.	82.8
0.033	0.001	0.222	0.046	0.245	0.165
6.636	6.635	6.680	6.642	6.692	6.676
0.609	0.581	0.805	0.558	0.731	0.607
5.118	5.131	5.031	5.145	5.070	5.129
17.0	17.0	17.0	17.0	17.0	17.0
-139.90	-139.90	-139.90	-139.90	-139.90	-139.90

TABLE 2

Pulsational Characteristics for Hydrogen-Poor Models.
(Asterisks indicate neglect of running waves.)

	$M = 15\ M_\odot$			
X_R	0.10	0.10	0.05	0.05
q_S	0.95	0.98	0.95	0.97
ω^2	4.044	3.403	3.546	3.076
Period (hr)	0.46	0.45	0.46	0.45
β_R	0.679	0.701	0.686	0.713
$\log \rho_R$	-7.149	-7.082	-7.064	-6.999
$\log g_R$	5.464	5.525	5.505	5.555
$(\delta r/r)_R$	1.000	1.000	1.000	1.000
$(\delta T/T)_R$	-2.205	-2.050	-2.075	-1.971
$(\delta L/L)_R$	-4.280	-4.199	-4.300	-3.885
$(\delta r/r)_S$	0.416	0.566	0.495	0.606
$(\delta T/T)_S$	-0.630	-0.887	-0.739	-0.921
$(\delta L/L)_S$	-0.510	-0.887	-0.607	-0.876
$(\delta r/r)_C$	0.320	0.422	0.384	0.467
$(\delta T/T)_C$	-0.369	-0.486	-0.443	-0.539
L^S_{PN}/L	0.69	0.00	0.89	0.06
L^C_{PN}/L	3.199	6.085	4.504	7.448
L_{PN}/L	3.89	6.09	5.40	7.50
L^e_{PH}/L	6.613	5.416	5.591	4.843
L^C_{PH}/L	0.121	0.219	0.174	0.269
L_{PH}/L	6.734	5.636	5.765	5.112
L_{PS}/L	1.129	1.105	1.092	1.122
L_P/L	-3.97	-0.65	-1.46	1.27
L^*_P/L	-2.85	0.45	-0.37	2.39
$1/K$ (yr)	-725	-7860	-2730	+4930
$1/K^*$ (yr)	-1010	+11300	-10100	+2620

TABLE 2 (continued)

M = 60 M⊙					
0.15	0.15	0.15	0.10	0.05	0.05
0.80	0.95	0.98	0.95	0.90	0.95
6.521	3.505	2.828	2.866	5.507	2.235
5.07	0.98	0.95	0.97	1.34	0.96
0.268	0.350	0.356	0.363	0.290	0.386
-8.680	-7.700	-7.632	-7.590	-7.936	-7.453
4.140	5.274	5.353	5.338	4.959	5.417
1.000	1.000	1.000	1.000	1.000	1.000
-2.652	-1.906	-1.735	-1.746	-2.401	-1.590
-6.610	-3.624	-2.940	-2.985	-5.603	-2.359
0.009	0.369	0.524	0.480	0.088	0.608
-0.014	-0.473	-0.682	-0.604	-0.129	-0.751
-0.001	-0.186	-0.355	-0.245	-0.026	-0.315
0.005	0.301	0.417	0.395	0.060	0.508
-0.006	-0.320	-0.443	-0.419	-0.064	-0.539
0.00	0.22	0.00	0.37	0.09	0.63
0.000	2.262	4.487	3.767	0.069	6.190
0.00	2.48	4.49	4.13	0.16	6.82
10.534	4.482	3.374	3.462	8.234	2.538
0.000	0.047	0.113	0.081	0.001	0.135
10.534	4.530	3.488	3.542	8.235	2.672
0.271	0.511	0.450	0.474	0.533	0.439
-10.80	-2.56	0.55	0.12	-8.61	3.71
-10.53	-2.04	1.00	0.59	-8.08	4.15
-0.858	-488	+4170	+17400	-12.2	+885
-0.880	-610	+2290	+3460	-13.0	+792

TABLE 2 (continued)

$M = 100\ M_\odot$					
0.15	0.15	0.10	0.10	0.05	0.05
0.95	0.97	0.90	0.95	0.90	0.93
3.295	2.847	5.855	2.401	4.655	3.015
1.26	1.23	1.86	1.23	1.61	1.30
0.263	0.265	0.219	0.285	0.235	0.262
-7.879	-7.835	-8.215	-7.720	-8.024	-7.785
5.219	5.275	4.826	5.322	4.974	5.223
1.000	1.000	1.000	1.000	1.000	1.000
-1.839	-1.726	-2.477	-1.616	-2.178	-1.768
-3.354	-2.903	-5.908	-2.464	-4.710	-3.071
0.368	0.465	0.054	0.533	0.143	0.394
-0.453	-0.576	-0.077	-0.642	-0.193	-0.488
-0.140	-0.215	-0.010	-0.210	-0.035	-0.134
0.307	0.384	0.038	0.452	0.106	0.323
-0.321	-0.402	-0.040	-0.473	-0.111	-0.338
0.15	0.01	0.02	0.36	0.16	0.62
2.282	3.696	0.03	4.900	0.213	2.231
2.43	3.71	0.05	5.27	0.37	2.85
4.053	3.349	8.895	2.721	6.415	3.609
0.037	0.069	0.000	0.081	0.003	0.033
4.090	3.418	8.895	2.802	6.417	3.641
0.442	0.403	0.492	0.391	0.486	0.431
-2.10	-0.12	-9.33	2.07	-6.53	-1.22
-1.66	0.29	-8.84	2.46	-6.05	-0.79
-537	-14800	-5.69	+1140	-32.4	-999
-680	+5930	-6.01	+957	-35.0	-1540

TABLE 3

Critical Models Dividing Stable from

Unstable Models

	7–8 M$_\odot$	15 M$_\odot$		60 M$_\odot$			100 M$_\odot$		
X_R	...	0.10	0.05	0.15	0.10	0.05	0.15	0.10	0.05
q_s	1.00	0.98	0.96	0.98	0.95	0.94	0.97	0.94	0.94
q_s^*	1.00	0.98	0.95	0.97	0.94	0.93	0.97	0.94	0.93
ω^2	3.6	3.3		2.9			2.8		
Period (hr)	0.30	0.45		0.97			1.23		
$\rho_c/\bar{\rho}$	20	27		54			69		

FIGURE CAPTION

Fig. 1. - Theoretical H-R diagram for superluminous massive stars.

Filled circles are Wolf-Rayet stars as located by Rublev.

Open circles represent our models, including unstable mo-

dels (crossed open circles). The stars are bounded on the

left and right by the pure helium sequence and normal main

sequence, respectively; several masses (solar units) are

indicated.